CLINICAL REPORT

Susceptibility-Weighted Imaging: A New Tool in the Diagnosis and Evaluation of Abnormalities of the Vein of Galen in Children

B.D. Jagadeesan
D.T. Cross III
J.E. Delgado Almandoz
C.P. Derdeyn
D.N. Loy
R.C. McKinstry
T.L.S. Benzinger
C.J. Moran

SUMMARY: We retrospectively identified 9 consecutive children, 3 males and 6 females (age 5.2 ± 6.3 years, range 1 day to 18 years), with known or suspected AVGs who underwent MR imaging, including SWI, at our institution between January 2007 and March 2011. On the SWI sequence, arterialized blood flow was considered to be present in the vein of Galen or its tributaries when these showed abnormal signal hyperintensity from arteriovenous shunting. SWI findings were correlated with findings from DSA studies or findings from time-of-flight or contrast-enhanced MR angiography sequences. SWI was found to accurately differentiate between high-flow and low-flow AVGs and was also useful in characterizing the arterial supply and venous drainage patterns associated with high-flow AVGs.

ABBREVIATIONS: AVG =abnormality of the vein of Galen; AVS = arteriovenous shunting; VGAD = vein of Galen aneurysmal dilation; VGAM = vein of Galen aneurysmal malformation

SWI is an MR imaging technique that combines both phase and magnitude signal to produce high-resolution images of the cerebral venous system.[1] In SWI, veins appear hypointense due to the presence of deoxyhemoglobin and the arteries are hyperintense due to time-of-flight effects and lack of T2* effects.[1,2]

It has recently been shown that this property of SWI could be used to accurately detect AVS in cerebral vascular malformations by identifying the presence of abnormal hyperintense signal within the veins draining these malformations; this high signal is a result of AVS and arterialized blood flow in these veins.[3] SWI studies are of high resolution and do not require intravenous contrast administration, features that can make these studies particularly useful in evaluating the presence of AVS in cerebral vascular malformations occurring in small children. We therefore retrospectively reviewed the utility of SWI in a series of patients with abnormalities of the vein of Galen. When there is AVS associated with such abnormalities, it could be from arteriovenous shunting into a persistent median vein of the prosencephalon (vein of Markowski), otherwise called a VGAM, or from a pial arteriovenous malformation that drains into the vein of Galen, resulting in a VGAD. In this context, we studied if the SWI technique could accurately differentiate between VGAMs and VGADs. When either of these high-flow abnormalities with AVS were identified by the SWI studies, we assessed the ability of these studies to provide information on the angioarchitecture associated with these abnormalities as well as their hemodynamic consequences.

Received May 12, 2011; accepted after revision November 15.

From the Section of Neuroradiology, Mallinckrodt Institute of Radiology (B.D.J., D.T.C., J.E.D.A., C.P.D., D.N.L., R.C.M., T.L.S.B., C.J.M.), and Departments of Neurological Surgery (D.T.C., C.P.D., C.J.M.) and Neurology (C.P.D.), Washington University, Saint Louis, Missouri.

Dr. Benzinger received support from the Bracco/American Roentgen Ray Society (ARRS) Scholar Award, the National Multiple Sclerosis Society (NMSS) RG 4190A2/1, and NIH R01 1RO1NS066905–01 and NIH/NIA AG003991–27 for this research.

Please address correspondence to Bharathi D. Jagadeesan, MD, Division of Neuroradiology, University of Minnesota, MMC 292, B226 E Mayo Memorial Building, 420 Delaware St SE, Minneapolis, MN 55435; e-mail: jagad002@umn.edu

http://dx.doi.org/10.3174/ajnr.A3058

Case Series

Patient Selection

The study was approved by our hospital's institutional review board and conducted in compliance with the Health Insurance Portability and Accountability Act. On a retrospective review of a prospectively maintained data base, we found that between January 1, 2007, and February 28, 2010, 9 children (6 females and 3 males, mean age 5.2 ± 6.3 years) underwent MR imaging with SWI at our institution for evaluation of known or suspected AVGs. All 9 patients also underwent TOF MRA and contrast-enhanced MRA studies as part of the same MR imaging study. Six of the 9 underwent DSA evaluation. The mean time interval between the MR imaging and DSA examinations was 212 ± 218.52 days (median 4 days, range 0–693 days). No patient underwent treatment in the time interval between the MR imaging and DSA studies. Two of the patients had intracranial hemorrhage at the time of presentation and 1 patient had a previously treated, known high-flow AVG. Both the MR imaging and DSA examinations were performed as part of standard of care procedures, and the decision to perform these examinations was at the discretion of the clinical providers.

Image Acquisition and Review of Medical Records

MR imaging studies were performed on either 1.5T or 3T scanners (Symphony 1.5T and Trio 3T; Siemens, Erlangen, Germany) and included the standard FDA-approved SWI sequence. At 1.5T, the SWI scanning parameters were flip angle, 15°; TE, 40 msec; TR, 50 msec; section thickness, 2.0 mm; and in-plane resolution of 1 × 1 mm. At 3T, the SWI scanning parameters were flip angle, 15°; TE, 20 msec; TR, 27 msec; section thickness, 2.0 mm; and in-plane resolution of 0.9 × 0.9 mm. Contrast-enhanced MRA was performed using standard vendor-provided sequences (Siemens). Postcontrast SWI was performed immediately after the end of the venous phase of the contrast-enhanced MRA sequence (when contrast-enhanced MRA was performed) and is otherwise identical to the routine precontrast SWI sequence in all respects.

Conventional angiography was performed using a dedicated biplanar neuroangiographic unit (Axiom Artis; Siemens), with transfemoral arterial access and intravenous conscious sedation, followed by selective catheterization and contrast injection (Optiray 320; Covidien, Hazelwood, Missouri) in the vessels of interest.

Two experienced neuroradiologists, blinded to the results of DSA, TOF MRA, contrast-enhanced MRA, and clinical characteristics, independently reviewed the SWI studies after multiplanar reformatting of the original transaxial sections. These images were reformatted and reviewed using the Emageon Ultravisual Viewer (Amicas, Boston, Massachusetts), embedded within our hospital's clinical information system (Clinical Desktop; BJC Health Care, St. Louis, Missouri), to assess for the presence of AVS, as determined by the presence of signal hyperintensity within the vein of Galen and its tributaries. When AVS was present, we attempted to further characterize the high-flow AVGs based on the pattern of arterial supply and the presence or absence of an associated AVM nidus with drainage into the vein of Galen. With regard to evaluation of the hemodynamic consequences of high-flow AVGs on the cerebral venous system, the presence of an abnormal hyperintense signal within enlarged deep veins or pial veins was used to identify reflux of arterialized blood from the vein of Galen into these veins. The presence of dilated hypointense cortical and deep venous channels was used to identify passive venous congestion. All differences in reader interpretation were resolved by consensus using a panel that included an additional board-certified neuroradiologist.

Subsequently, the DSA and MRA examinations were reviewed in conjunction with an experienced interventional neuroradiologist to correlate the findings from the SWI study with those from the contrast MRA study and the DSA studies, whenever the latter were available.

The contrast-enhanced MRA studies had previously been independently interpreted by board-certified neuroradiologists as part of routine clinical care.

Medical records were reviewed for patient age, sex, clinical symptoms at the time of presentation, time interval between the MR imaging and DSA examinations, hemorrhage on initial head CT images, and prior surgical or endovascular treatments for AVGs.

Accuracy of SWI for the Detection of AVS in the Vein of Galen

Two of the 9 patients had low-flow AVGs, with enlargement of the vein of Galen secondary to drainage from multiple developmental venous anomalies; the vein of Galen was hypointense on the SWI sequence in both patients. Seven patients had high-flow AVGs and the vein of Galen was hyperintense in all 7 on the SWI study. Overall, SWI was 100% accurate with sensitivity, specificity, positive predictive value, and negative predictive value of 100% in differentiating between high-flow and low-flow AVGs.

Utility of SWI in the Further Classification of High-Flow AVGs

Of the 7 patients with high-flow AVGs, 3 had VGAMs and 4 had VGADs. All 3 patients with VGAMs had choroidal-type VGAMs (using the classification proposed by Garcia-Monaco[4] and colleagues). SWI was 100% accurate in characterizing the above subtypes. In the 4 patients with VGAD, the AVM nidus was located in the left thalamus, left lateral ventricle choroid plexus, the surface of the left cerebral hemisphere, and the left temporal lobe, respectively.

Utility of SWI in the Evaluation of the Cerebral Hemodynamic Consequences of High-Flow AVGs

Two of the patients with high-flow AVGs showed diffuse cortical volume loss; in both patients, there was diffuse cortical venous congestion and the enlarged veins were well demonstrated on the SWI study. In 2 patients, there was unilateral left occipitotemporal volume loss; in both patients, there was cortical venous congestion, which involved only the affected lobes, and this was well demonstrated on the SWI study. In 2 patients, there was efferent drainage of arterialized blood from the vein of Galen to veins surrounding the midbrain and brain stem, with formation of multiple venous aneurysms; this phenomenon was not well visualized on the time-of-flight MRA but was well demonstrated by the SWI and contrast-enhanced MRA studies.

Discussion

The term AVG can be broadly used to describe any condition in which the vein is abnormally large or has abnormal morphology. High-flow AVGs result from AVS into the vein of Galen, whereas low-flow AVGs result from difficulty in venous outflow from the vein of Galen or from excessive venous inflow into the vein of Galen from developmental venous anomalies.[5] High-flow AVGs can present in children with congestive heart failure and failure to thrive, or can result in hemorrhage, seizures, ventriculomegaly, and death, depending upon the anatomy, flow, and the age of presentation.[6] Imaging techniques used in the evaluation of AVGs must be capable of differentiating between high-flow and low-flow AVGs, and they should also be able to provide exquisite information regarding the arterial supply and the venous drainage pattern associated with high-flow AVGs. Time-resolved dynamic contrast-enhanced MRA techniques are likely to offer the greatest detail, if performed with high temporal and spatial resolution; however, in neonates with AVGs, physiologic immaturity in renal function often precludes intravenous administration of gadolinium agents. In addition, the hyperdynamic circulation and congestive cardiac failure associated with high-flow AVGs in neonates and children also make time-resolved MRA challenging. In neonates and young children, the small size of the cerebral vessels also requires time-resolved MRA techniques to maintain a high spatial resolution while retaining high temporal resolution to comprehensively image very high-flow AVGs. In addition, with bolus timing methods, the test bolus dose of contrast by itself may account for a large fraction of the relatively small amount of permitted contrast doses in children.[7] Recently, Chooi et al[8] studied a set of 15 pediatric patients with MR DSA and found that the extremely high flow rates associated with AVGs resulted in poor visualization of the cerebral vessels other than the vein of Galen in these children. They also opined that the MR DSA results could not be used for treatment planning in these patients.

In this setting, a high-quality time-of-flight MRA has often been the study of choice; however, while time-of-flight imaging is excellent in the depiction of the arterial supply, it often does not reveal the venous drainage pattern in its entirety. In particular, it may not be useful in identifying passive cortical or deep venous congestion resulting from venous hypertension in patients with high-flow AVGs.

Recently, it has been shown that SWI can be used as an accurate method for the detection of arteriovenous shunt sur-

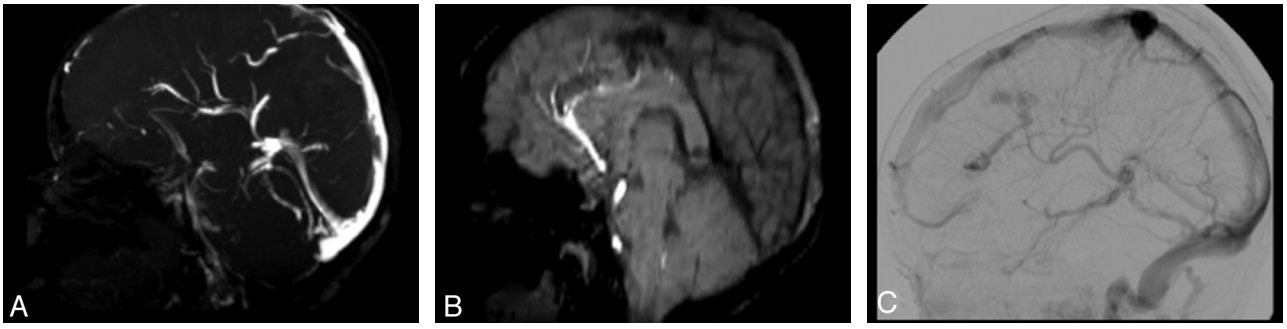

Fig 1. Images from a 3-year-old child with intracranial hemorrhage in utero and new onset aphasia. *A*, Sagittal time-of-flight MRA image shows an enlarged vein of Galen with mild prominence of the straight sinus. *B*, Sagittal reconstruction of an SWI image shows that the vein of Galen is entirely hypointense, suggesting that there is no arteriovenous shunt surgery. *C*, Lateral projection from the venous phase of a left common carotid artery injection during conventional catheter digital subtraction angiography shows an atypical frontal developmental venous anomaly draining into the vein of Galen.

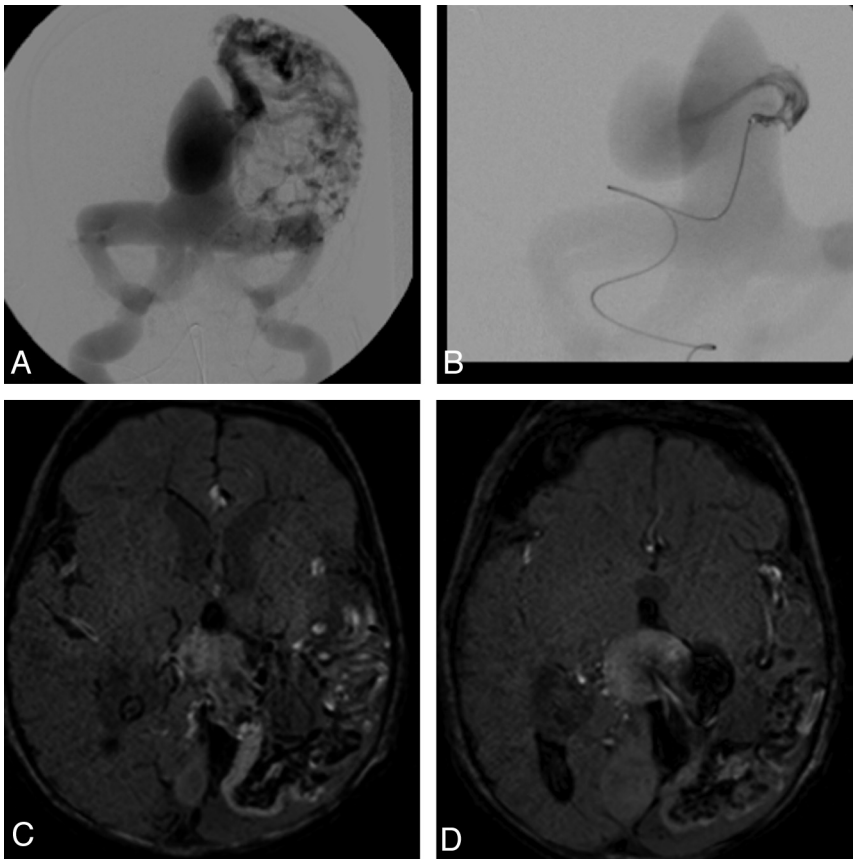

Fig 2. Images from a 4-week-old child with seizures. *A*, Postero anterior projection after left internal carotid artery injection during a DSA study shows an extensive arteriovenous malformation involving the entire left cerebral convexity, draining into the vein of Galen via a unique deep vein that drains the entire hemisphere. *B*, Postero anterior projection after microcatheter injection of a choroidal branch of the left posterior cerebral artery, showing that, in addition to the large draining vein from the cortical AVM, this malformation also has a fistulous communication with vein of Galen. *C*, Axial SWI image from the same patient shows hyperintense arterialized blood streaming into the vein of Galen from an enlarged draining vein. The extensive network of hyperintense vessels overlying the cerebral hemisphere corresponds to the large AVM seen on the DSA study. In addition, note the hypointense hemorrhagic blood products in the left parieto-occipital lobe. *D*, Axial SWI image at a different level also shows the fistulous component of this malformation with high signal intensity arterial blood streaming into the venous sac.

gery in complex brain vascular malformations.[3] George et al[9] also recently described the utility of SWI in the evaluation of brain arteriovenous malformations and used the magnitude images from the SWI studies to differentiate between the components of AVMs. This technique does not involve the administration of intravenous contrast or technically demanding bolus timing triggered acquisition or dynamic postcontrast image acquisition MR angiography techniques, which sacrifice spatial resolution for improvements in temporal resolution. These factors suggested to us that SWI might offer an alternative and promising technique for evaluating cerebral vascular malformations in children, including AVGs.

In this study, we found that the SWI images did indeed allow for differentiation between low-flow and high-flow AVGs. The 2 children with low-flow AVGs included in our study had undergone a subsequent DSA examination (Fig 1), with its added radiation exposure and other risks. If the SWI sequence is found to be reliable in its ability to identify such

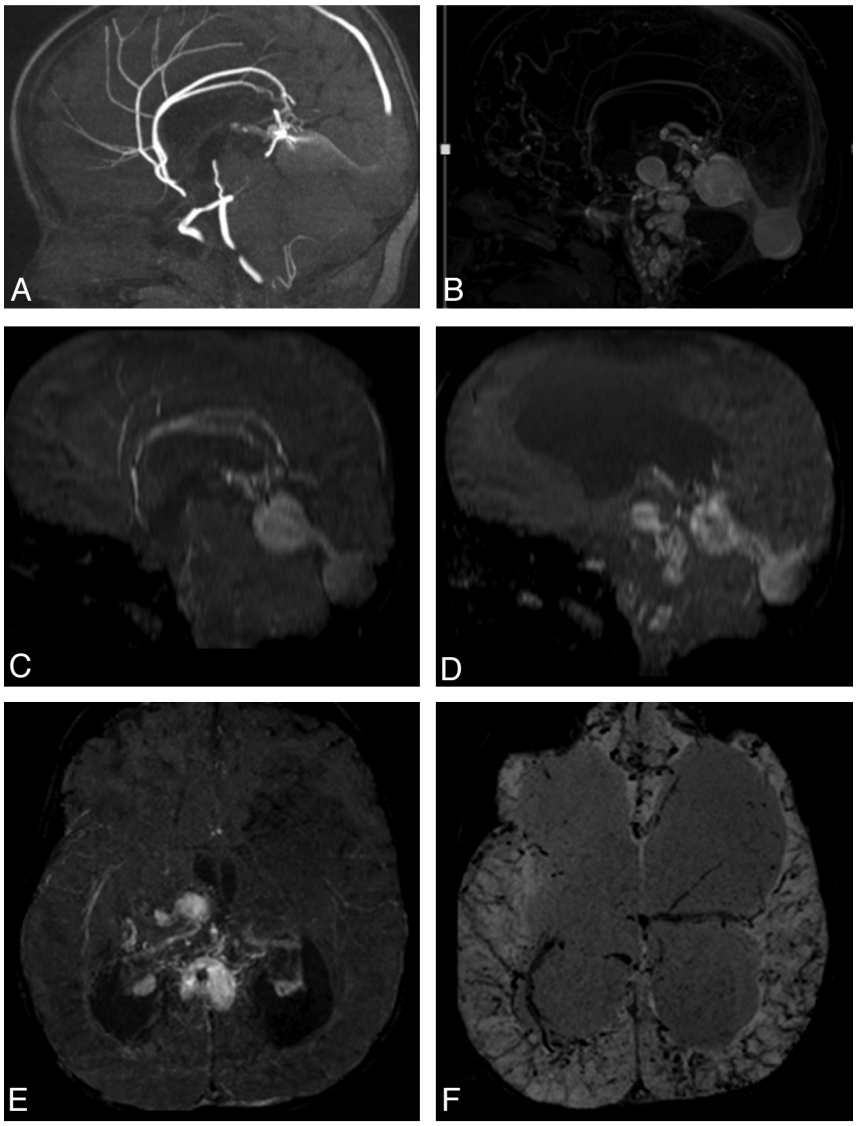

Fig 3. Images from a 3-month-old child with congestive cardiac failure. *A,* Sagittal image from a time-of-flight MRA study showing a choroidal-type VGAM with arterial supply from the branches of the anterior cerebral artery and posterior choroidal arteries. There is, however, not much information about the venous drainage pattern from the VGAM. *B,* Sagittal image from a contrast-enhanced MR angiogram showing multiple venous varices draining the vein of Galen and surrounding the brain stem. *C* and *D,* Sagittal reconstructions from SWI studies in the same child clearly show both the arterial feeders and the venous aneurysms associated with this VGAM. Axial maximal intensity projection image (*E*) and minimum intensity projection image (*F*) obtained from a postcontrast SWI dataset in the same patient show the hyperintense blood flow in the venous aneurysms around the brain stem (*E*) and the hypointense passive venous congestion in the deep and cortical veins (*F*). Note the associated ventriculomegaly in this child.

low-flow AVGs in a larger set of patients, such DSA examinations may be avoided in the future.

In children with high-flow AVGs, SWI studies enabled clear differentiation between different subtypes and also showed excellent depiction of the arterial supply to these malformations (Figs 2 and 3). Although DSA studies are ultimately necessary, we occasionally delay these in very young children with VGAMs who are asymptomatic, or who have manageable congestive cardiac failure, until such a time when they have achieved a body weight that will allow for adequate iodinated contrast volume to perform a comprehensive DSA study. In these children, the information obtained from the SWI may be used to limit DSA contrast, eliminating nonessential contrast injections during diagnostic DSA or therapeutic endovascular procedures. This may also enable us to perform the DSA examinations at an earlier age with less contrast.

This review of the SWI in children with VGAMs also allowed us to study the pattern of venous drainage from these malformations; we could differentiate between venous dilation resulting from passive congestion and venous dilation resulting from AVS. On the SWI, we found diffuse passive venous congestion in medullary and cortical veins in 2 of our patients with VGAMs. It has been suggested that such congestion may play a role in the development of ventriculomegaly in children with VGAMs.[10,11] Interestingly, both of the patients with diffuse medullary and cortical venous congestion also had diffuse cerebral volume loss and ventriculomegaly. In contrast to this phenomenon, in 2 patients with VGAMs, we also found that the multiple dilated veins surrounding the brain stem actually carried arterialized efferent flow from the malformation, as they were hyperintense on the SWI sequence. In 1 patient, there were multiple prominent venous

aneurysms surrounding the brain stem as a result of this phenomenon. The presence of these efferent pial venous drainage pathways carrying arterialized blood may impact upon the method and approach to treatment of these malformations,[12] and it is therefore important to differentiate them from veins enlarged because of passive venous congestion. These observations on the utility of SWI in differentiating between passive venous congestion and venous dilation from AVS in our series of patients are similar to the observations reported by Letourneau-Guillon and Krings[13] in their recent small series of patients with dural arteriovenous fistulas.

Recently, we have started performing our SWI studies after administration of intravenous gadolinium contrast in adult patients with cerebral arteriovenous malformations; the arteriovenous contrast in the SWI is further increased by intravenous gadolinium.[14] In the 1 patient included in this study who did have the SWI before and after intravenous contrast, the arterial and venous anatomy was better depicted on the postcontrast SWI study (Fig 3*E*, -*F*). This phenomenon may also be worth exploring further in children who are able to tolerate intravenous gadolinium, as the postcontrast SWI sequence can be performed after contrast equilibration and does not require dynamic imaging or bolus timing.

Although these findings show a promising role for the SWI technique in the evaluation of AVGs, our series suffers from the following limitations: First and foremost, the small number of patients included in this series, and the retrospective identification of the patients included in it, make it difficult to generalize our findings to a larger series of patients with AVGs. Second, the utility of SWI in the follow-up imaging of patients with treated AVGs, especially those treated with coil embolization, and the usefulness of SWI in the imaging of children who present with intracranial hemorrhages associated with AVGs is not clear. In this study, 2 patients had previously treated AVGs, and though we did not encounter any significant problems in image interpretation in these patients, we would need to study a larger number of patients with previously treated AVGs to identify any potential pitfalls. Likewise, in this study, the presence of hemorrhagic blood products (which were found in the vicinity of 2 of the high-flow AVGs) also did not interfere with our ability to differentiate between VGAMs and VGADs, but we would need to study a larger number of patients with intracranial hemorrhages using SWI to identify any potential pitfalls. Third, we did not obtain DSA data in all our patients, and in some patients, we used contrast-enhanced MRA as the reference standard. A future study comparing SWI results with DSA results in a larger number of patients will be necessary to fully establish the role of the SWI technique in AVGs.

Conclusions

Susceptibility-weighted imaging is a novel imaging technique that may provide useful morphologic and hemodynamic information in the evaluation of AVGs. It may potentially help in the classification of these rare malformations. In addition, it may serve as a useful supplementary technique to DSA and as an alternative to conventional MR angiography techniques in efforts to study the cerebrovascular hemodynamic consequences of these malformations in very young children.

Disclosures: Dr. Benzinger has previously served on the Siemens speakers' bureau, where she received support for travel (no fee). OTHER DISCLOSURES: Tammi Benzinger—*UNRELATED: Expert Testimony:* Kujawski and Associates, P.C.; *Grants/Grants Pending:* NIH/NIA*, National Multiple Sclerosis Society*, NIN/NINDS*. Christopher Moran—*RELATED: Consulting Fee or Honorarium:* eV3, Codman; *UNRELATED: Consultancy:* eV3, Codman, Comments: Procedure proctor, speaker; *Grants/Grants Pending:* Stryker*; *Payment for Lectures (including service on speakers bureaus):* eV3, Codman. (**Money paid to institution.*)

References

1. Haacke EM, Mittal S, Wu Z, et al. **Susceptibility-weighted imaging: technical aspects and clinical applications, part 1.** *AJNR Am J Neuroradiol* 2009;30:19–30
2. Barnes SRS, Haacke EM. **Susceptibility-weighted imaging: clinical angiographic applications.** *Magn Reson Imaging Clin N Am* 2009;17:47–61
3. Jagadeesan BD, Delgado Almandoz JE, Moran CJ, et al. **Accuracy of susceptibility-weighted imaging for the detection of arteriovenous shunting in vascular malformations of the brain.** *Stroke* 2011;42:87–92
4. Garcia-Monaco R, Lasjaunias P, Berenstein A. **Therapeutic management of vein of Galen aneurismal malformations.** In: Vinuela F, Halbach VV, Dion JE, eds. *Interventional Neurodadiology: Endovascular Therapy of the Central Nervous System*. New York: Raven Press, 1992:113–27
5. Gupta AK, Varma DR. **Vein of Galen malformations: review.** *Neurol India* 2004;52:43–53
6. Gold AP, Ransohoff J, Carter S. **Vein of Galen malformation.** *Acta Neurol Scand* 1964;40:1–31
7. Muthupillai R, Vick GW, Flamm SD, et al. **Time-resolved contrast-enhanced magnetic resonance angiography in pediatric patients using sensitivity encoding.** *J Magn Reson Imaging* 2003;17:559–64
8. Chooi WK, Connolly DJA, Coley SC, et al. **Assessment of blood supply to intracranial pathologies in children using MR digital subtraction angiography**. *Pediatr Radiol* 2006;36:1057–62
9. George U, Jolappara M, Kesavadas C, et al. **Susceptibility-weighted imaging in the evaluation of brain arteriovenous malformations.** *Neurol India* 2010;58:608–14
10. Zerah M, Garcia-Monaco R, Rodesch G, et al. **Hydrodynamics in vein of Galen malformations.** *Childs Nerv Syst* 1992;8:111–17
11. Di Rocco C. **Vein of Galen aneurysm and hydrocephalus.** *Childs Nerv Syst* 1991;7:359
12. Pearl M, Gomez J, Gregg L, et al. **Endovascular management of vein of Galen aneurysmal malformations. Influence of the normal venous drainage on the choice of a treatment strategy.** *Childs Nerv Syst* 2010;26:1367–79
13. Letourneau-Guillon, Krings T. **Simultaneous arteriovenous shunting and venous congestion identification in dural arteriovenous fistulas using susceptibility-weighted imaging: initial experience.** *AJNR Am J Neuroradiol* 2012;33:301–07
14. Jagadeesan BD, Delgado Almandoz JE, Benzinger TL, et al. **Postcontrast susceptibility-weighted imaging: a novel technique for the detection of arteriovenous shunting in vascular malformations of the brain.** *Stroke* 2011;42:3127–31